Can Genotypic Differences in Rice Response to Elevated CO 2 be Predicted with Proxy Traits Measured under Ambient CO 2 Levels?

michael dingkuhn[1], Denis Fabre[1], Apolline Chemier[1], Gregory Aguillar[1], Sandrine Roques[1], and Xinyou Yin[2]

[1]CIRAD Departement Systemes biologiques
[2]Wageningen University & Research Plantenwetenschappen

June 2, 2023

Abstract

Rising atmospheric [CO $_2$] causes global warming but may also benefit photosynthesis and yield of C3 crops such as rice. Previous research showed that positive effects depend on a cultivar's sink-source ratio as sink limitation incurs acclimation of photosynthesis to elevated [CO $_2$] (e-CO $_2$). To enable breeding for e-CO $_2$ response, predictive, easily measurable proxy traits under ambient [CO $_2$] are needed. The local source-sink ratio (LSSR: flag leaf/panicle size) is a potential proxy trait, proposed by a previous study. We evaluated this and similar trait indices for two diverse rice cultivar samples under e-CO $_2$ vs ambient level in controlled environments. The significant negative effect of genotypic LSSR on maximum photosynthesis (A_{max}) under e-CO $_2$, and a similar but weaker effect on the grain yield response, was confirmed. However, LSSR observed was more predictive under e-CO $_2$ than ambient, rendering this proxy trait impractical for field-based selection. This difference was due to the phenotypic plasticity of LSSR between [CO $_2$] levels in our populations. Variants of LSSR incorporating SPAD leaf chlorophyll content and panicle sink capacity improved LSSR predictive power under ambient [CO $_2$] for A_{max}. We conclude that genotypic sink-source ratio is an important physiological determinant of [CO $_2$] response, but proxy traits need to be further refined and field-validated to become useful selection or phenotyping tools for improved e-CO $_2$ response of rice.

Title:

Can Genotypic Differences in Rice Response to Elevated CO_2 be Predicted with Proxy Traits Measured under Ambient CO_2 Levels?

Authors:

Denis Fabre[1], Apolline Chemier[1], Gregory Aguillar[1], Sandrine Roques[1], Xinyou Yin[2], Michael Dingkuhn[1*]

Contact information

[1]CIRAD, UMR AGAP Institut (Univ Montpellier – CIRAD – INRAE - Institut Agro), Montpellier 34398, France.

[2]Centre for Crop Systems Analysis, Dept. Plant Sciences, Wageningen University & Research, Wageningen, The Netherlands.

*Corresponding author

Corresponding author

Michael Dingkuhn

CIRAD, UMR AGAP, F-34398 Montpellier, France

<*michael.dingkuhn@cirad.fr*>

Abstract

Rising atmospheric [CO_2] causes global warming but may also benefit photosynthesis and yield of C3 crops such as rice. Previous research showed that positive effects depend on a cultivar's sink-source ratio as sink limitation incurs acclimation of photosynthesis to elevated [CO_2] (e-CO_2). To enable breeding for e-CO_2response, predictive, easily measurable proxy traits under ambient [CO_2] are needed. The local source-sink ratio (LSSR: flag leaf/panicle size) is a potential proxy trait, proposed by a previous study. We evaluated this and similar trait indices for two diverse rice cultivar samples under e-CO_2 vs ambient level in controlled environments. The significant negative effect of genotypic LSSR on maximum photosynthesis (A_{max}) under e-CO_2, and a similar but weaker effect on the grain yield response, was confirmed. However, LSSR observed was more predictive under e-CO_2 than ambient, rendering this proxy trait impractical for field-based selection. This difference was due to the phenotypic plasticity of LSSR between [CO_2] levels in our populations. Variants of LSSR incorporating SPAD leaf chlorophyll content and panicle sink capacity improved LSSR predictive power under ambient [CO_2] for A_{max}. We conclude that genotypic sink-source ratio is an important physiological determinant of [CO_2] response, but proxy traits need to be further refined and field-validated to become useful selection or phenotyping tools for improved e-CO_2 response of rice.

Key words

Oryza sativa L., Sink-source ratio, A_{max}photosynthesis, CO_2 acclimation, crop CO_2 response, climate change

Introduction

While climate change is considered to have mostly adverse effects on crop production through heat stress (Zhao et al. 2017) and heat spells, rising nocturnal temperatures (Jagadish *et al.* , 2015, 2016; Sadok and Jagadish, 2020; Impa *et al.* , 2021), more frequent periods of drought or floods (Rohde, 2023), and more variable climatic conditions in general, the rise of atmospheric CO_2 concentration ([CO_2]) may have beneficial effects. For photosynthesis of C3 plants such as rice, CO_2 is a limiting resource, and free-air CO_2 enrichment experiments (FACE) in Japan (Hasegawa *et al.* , 2013, 2016; Kumar*et al.* , 2017) and China (Liu *et al.* , 2017; Cai *et al.* , 2020; Lv *et al.* , 2020) have established that yield gains are substantial under an increase of [CO_2] from current levels (around 400 µmol mol^{-1}) to those expected for 2050 (550 to 600 µmol mol^{-1}). The same studies indicated that varietal differences are large for this response.

Dingkuhn et al. (2020) reviewed the probable physiological causes of varietal differences in CO_2 response in C3 crops. A major determinant is the carbon sink capacity that should be commensurate with the increased source under elevated [CO_2] (e-CO_2). Thus, breeding for optimum C source-sink relationships might provide gains in photosynthesis response to e-CO_2 and thereby increase biomass and yield.

Comparing various rice genotypes having contrasting local source-sink ratio (LSSR), defined as the ratio between flag leaf area and grain number of the adjacent panicle on the main stem, Fabre et al. (2019 & 2020) demonstrated that this trait is related to rice yield and photosynthetic response to e-CO_2. Genotypes with larger sink capacities during grain filling (low LSSR) benefited more from CO_2 enrichment while having increased photosynthetic capacity (A_{max}) of flag leaves. Under severe sink limitation caused by panicle pruning and e-CO_2treatment, triose-phosphate utilization (TPU) was identified as the main biochemical driver of photosynthesis down-regulation, also called acclimation (Fabre *et al.* , 2019, 2020; McClain *et al.* , 2023). Down-regulation of A_{max} mainly occurred in the afternoon. A negative correlation was found between TPU and markers of sink limitations, such as leaf sucrose accumulation and LSSR. It is becoming increasingly evident that ignoring TPU in situations of source-sink imbalance can cause errors when modeling crop photosynthesis (Sharkey, 2019; Yin *et al.* , 2021)

A consequence of these findings is that A_{max} is not solely determined by constitutive properties of the photosynthetic apparatus of a given plant, in which case its value would be constant during the day. Instead, A_{max} decreases throughout the day, particularly when the local carbon source-sink ratio is high (Fabre

and Dingkuhn, 2022). This indicates that maintaining high A_{max} requires efficient evacuation of photosynthates from the leaves. This has consequences for strategies to improve plants for growing under future e-CO_2environments.

Given that photosynthesis and yield response to e-CO_2can be substantial and is in large part genotypic in rice (FACE trials: Hasegawa et al., 2013; Lv et al., 2020), this trait can be potentially enhanced by breeding. Breeding now for this trait, however, would be unrealistic if requiring selecting for the trait under e-CO_2 conditions, as FACE experiments are expensive, limited in size allowing to test only a small number of genotypes, and available for rice at only a few sites worldwide. The same applies to indoor controlled environments, which in addition would be unacceptable to breeders. The true source-sink ratios during grain filling are difficult to measure. This situation calls for the identification of more easily measurable proxy traits for showing e-CO_2response if they exist. If a genotype's morphological sink-source ratio is indeed a major physiological determinant of e-CO_2response and sufficiently constitutive to be conserved across different CO_2 levels, predictive proxy traits might indeed be found. The LSSR (Fabre *et al.* , 2020) may be such a trait, although it was proposed, based on the experimental results in only a small set of rice varieties.

The LSSR is only a crude indicator. On the source side, the flag leaf, although the most light-exposed and located close to the panicle, represents only a fraction of the plant's photosynthetic potential. Furthermore, its specific leaf area (SLA) and chlorophyll and nitrogen content also contribute to photosynthetic potential (Seneweera *et al.* , 2011; Xiong *et al.* , 2015; Wang *et al.* , 2022) and are not captured by LSSR. On the sink side, the panicle's spikelet number is widely considered a measure of its overall sink capacity (Sheehy *et al.* , 2001; Fabre *et al.* , 2016; Nakano *et al.* , 2017; Mai *et al.* , 2021) but does not inform on the current sink strength of any given spikelet, nor does it take into account the genotypic variation of the attainable grain weight. There may thus be room to improve LSSR as an indicator of a rice plant's source-sink ratio.

The present study aims at i) validating LSSR as a potential proxy trait to predict rice genotypic photosynthetic and yield response to e-CO_2 for larger samples of cultivars; and ii) exploring possible improvements of the proxy trait, in terms of predictive power and practical considerations for plant selection or phenotyping. We present the results of controlled-environment experiments and discuss them with respect to further research needed to enable breeding for improved rice CO_2 response.

Materials and Methods

Plant material and growth conditions

Two experiments were conducted to investigate the diversity of local C source–sink ratio and its impact on rice photosynthetic and yield response to e-CO_2. Exp. 1 was conducted in growth chambers, while Exp. 2 was a more detailed trial conducted in a climate-controlled greenhouse. The trials used different but partially overlapping sets of genotypes (Table 1). They were selected to represent diversity in local C source–sink ratio (LSSR), based on previous field phenomics data provided by CIAT in Colombia (Rebolledo *et al.* , 2016). The selection of genotypes also attempted to limit other sources of variation, such as degree-days to flowering, tiller and panicle numbers per plant, plant height and spikelet fertility.

Genotypes were germinated on wet filter paper and transplanted into 6-L pots filled with Jiffy substrate, pH4.5 (Jiffy Products International BV*)* . This pot size is sufficient for rice to avoid reductions in photosynthesis or biomass accumulation along plant cycle (Poorter et al., 2012; Sage, 1994). Basal fertilizer was applied before transplanting using a mixture of Basacot 6 M high (Compo Expert, France), 13%N–5%P–18%K and Siforga (MeMon BV), 5%N–3%P–8%K at 2 g l^{-1}. A second application at 2 g l^{-1} was performed just before heading stage to avoid post-floral nitrogen deficiency.

Exp. 1: Plants were grown from March to July 2021 at the Agronomical Research and International Center for Development (CIRAD, Montpellier, France) in two adjacent fully climate controlled walk-in growth chamber, ARALAB FITOCLIMA 25.000HP located in CIRAD's*AbioPhen*platform for climate change studies. They were grown under artificial light provided by Philips full spectrum ceramic metal halide (CDM-TMW 315W/930 1CT) providing on average photosynthetic irradiance of 800 µmol m^{-2} s^{-1} at the top of the canopy

level during a 12-h photoperiod. Air temperature was set to 28° C (day) and 22° C (night). Air relative humidity was set to 65% (day) and 80% (night). The two chambers were differentiated by the atmospheric CO_2 level applied from transplanting to maturity: 400 µmol mol^{-1} (ambient) versus 700 µmol mol^{-1} (e-CO_2).

Exp. 2 : Plants were grown from March to July 2022 in the same building as EXP1 (*AbioPhen* complex) in two adjacent, climate-controlled greenhouse compartments. They were grown under natural daylight with supplemental lighting maintaining a 12-h photoperiod using horticultural red-blue LED projectors (Alpheus Radiometrix 15M1006) providing R/FR ratio of about 1.2. Microclimate was monitored using data loggers (CR1000 Campbell Scientific) installed in each compartment. Air temperature averaged 27°C (day) and 21°C (night) as measured with a PT1000 probe under fan-aspirated shield. Air relative humidity averaged 65% (day) and 75% (night), measured by HMP45 (Vaisala, Helsinki, Finland), and photosynthetic photon flux density (PPFD) was measured with a SKP215 (Skye Instrument quantum sensor, Powys, UK) providing on average photosynthetic irradiance of 800 µmol m^{-2} s^{-1} at the top of the canopy level during the daytime. The mean photosynthetically active radiation received by the plants during their life cycle was 7.58 MJ m^{-2} d^{-1}. The two compartments were differentiated by the atmospheric CO_2 level applied from transplanting to maturity: 400 µmol mol^{-1} versus 650 µmol mol^{-1}.

In both experiments, all the pots (including a row of border plants) were arranged at 20 cm spacing among plants in a randomized design with four replications per cultivar and per CO_2 treatment on movable tables. Pots were kept watered at field capacity while maintaining the perforated pot bottoms in 5 cm of standing water. To minimize border effects on each table, border plants on the tables were not used for measurements. The tables were moved weekly to avoid the effects of spatial heterogeneity.

For each CO_2 treatments, plants were characterized for growth and development traits along the cycle, photosynthesis and biochemical measurements at 15 days after heading, final biomass and grain production as described hereafter, whereas EXP1 has focused only on the photosynthesis measurement at 15 days after heading.

Leaf photosynthesis measurement

Photosynthesis measurements were performed *in situ* on the fully expanded flag leaf on the main stem of four plants per cultivar in each treatment, 2 weeks after heading. Comparison between the CO_2 treatments was made by using an infrared gas analyzers (Li-Cor 6800F; Li-Cor Inc., Lincoln, NE, USA). The leaf photosynthesis rate under saturating light (1,500 µmol m^{-2}s^{-1}) and CO_2 levels (1,600 µmol mol^{-1}) was taken using the 6 cm^{2}chamber, as the maximum leaf photosynthesis capacity level ($A_{\max}$). All the measurements were carried out at a leaf temperature of 25 °C, relative humidity in the cuvette set to 65%, with a flow rate of 700 µmol s^{-1}. The steady-state fluorescence yield (Fs) was measured just after registering the gas-exchange parameters, and a saturating light pulse of 8000 µmol m^{-2} s^{-1} was applied to achieve the light-adapted maximum fluorescence (Fm'). The operating PSII photochemical efficiency (φPSII) was determined as (1-Fs/Fm'), and then ETR was calculated (Table S1). To minimize the confounding effect of diurnal trends in photosynthesis downregulation related to C sink limitations, previously observed to increase along the day (Fabre*et al.* , 2019), all measurements were made at least 6 hours after onset of the light period (afternoon). This served to capture effects of photosynthetic acclimation, if any.

Then, the ratio of the average $A_{\max}$ of plants grown at e-CO_2 by the average$A_{\max}$ of plants grown at ambient CO_2 ($A_{\max}$ e-CO_2 /$A_{\max}$ ambient) was calculated.

A relative indicator of chlorophyll content (SPAD) was measured on the same leaf using a SPAD-502 (Minolta, Ltd., Japan). In EXP2, specific leaf area (SLA [cm^2 g^{-1}]) was determined in addition, on the flag leaf used for gas exchange measurements. The area of each leaf was measured with a leaf area meter (Li-Cor 3100, Lincoln, NE, USA) and the leaf then oven-dried until constant weight (48 hr at 70°C).

Sugar Content Analysis

Immediately after photosynthesis measurement, the same leaf was sampled to determine non-structural carbohydrate content (NSC: starch, sucrose, glucose and fructose). Prior to grinding with a ball grinder

(Mixer mill MM 200, Retsch, Germany), the samples were frozen in liquid nitrogen. The sugars were extracted three times from 20 mg samples with 1 ml of 80% ethanol for 30 min at 75°C and then centrifuged for 10 min at 9500 g (Mikro 200, Hettich centrifuge). Soluble sugars (sucrose, glucose and fructose) were contained in the supernatant and starch in the sediment. The supernatant was filtered in the presence of polyvinyl polypyrrolidone and activated carbon to eliminate pigments and polyphenols. After evaporation of solute with Speedvac (RC 1022 and RCT 90, Jouan SA, Saint Herblain, France), soluble sugars were quantified by high-performance ionic chromatography (HPIC, standard Dionex) with pulsed amperometric detection (HPAE-PAD). The sediment was solubilized with 0.02 N NaOH at 90°C for 1hr 30 min and then hydrolyzed with a-amyloglucosidase at 50°C and pH 4.2 for 1 hr 30 min. Starch was quantified as described by Boehringer (Pomeranz and Meloan, 1994) with 5 µl of a mixture of hexokinase and glucose-6-phosphate dehydrogenase (HK/G6P-DH Sigma Aldrich), followed by spectrophotometry of NADPH at 340 nm (spectrophotometer UV/VIS V-530, Jasco Corporation, Tokyo, Japan).

Plant Growth, Biomass and Yield Component Measurements

At maturity stage, plant shoots were harvested. The panicles were counted, and the total stem and leaf dry matter per plant (Tot.shoot dry matter) were measured after drying at 70°C for 48 h and adding DM from organs used for biochemical analyses. Maximum tiller number was determined at vegetative stage.

Grain yield and yield components were calculated according to (Liu*et al.* , 2008): grains were sorted by using a densiometric column. The dry weight of ripened grains was determined after oven-drying at 80°C for 72 h. The 1,000-grain dry weight was then calculated.

In both experiments, local C source–sink ratio (LSSR) was estimated for each plant by dividing flag leaf blade area and fertile spikelet number on the main stem.

Statistical analysis

Physiological, biochemical traits and yield components were analyzed as a completely randomized design using a two-way analysis of variance of CO_2 treatment, genotype and interaction using XLSTAT after testing for normal distribution. Wherever appropriate, comparison between means was performed using Tukey's post hoc test ($\alpha = 0.05$). Principal component analysis (PCA) was performed using the FactoMineR package using R (version 4.2.2, R Foundation for Statistical Computing) to analyze covariation.

Table 1. List of genotypes in Exp.1 and Exp.2

Cultivar Exp1	Cultivar Exp2	Origin	Genetic group	Type
V01	IRRI147	IRRI147	Philippines	*O. sativa* indica Improved
V02				

Results

Exp. 1: LSSR predicts genotypic CO_2response only when measured at elevated CO_2

Fabre et al. (2020) proposed on the basis of 5 rice genotypes that LSSR may be a predictive proxy trait for A_{max} response to elevated CO_2. Exp. 1 was conducted to confirm this effect for 14 genotypes (which include 2 of the 5 genotypes used by Fabre et al. 2020; Table 1). As Fig. 1 demonstrates, the observed A_{max} ratio between elevated and ambient CO_2 levels was significantly ($P<0.01$), negatively correlated with LSSR measured under elevated CO_2, but not with LSSR measured at the ambient CO_2 level. The more detailed study Exp. 2 was therefore conducted to better understand parameter relationships for a partially overlapping but more diverse sample of genotypes.

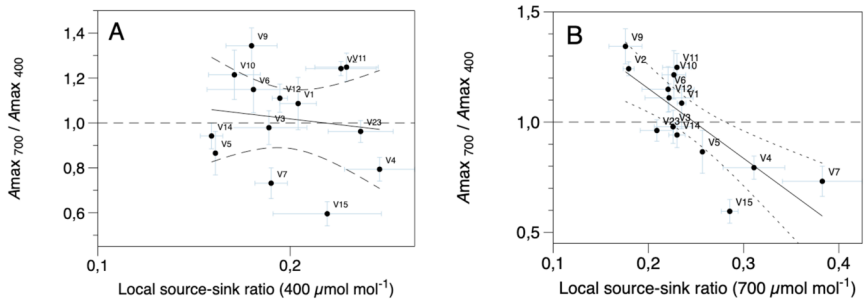

Fig. 1. Genotypic response of flag leaf $A_{\max}$ **το ελεατεδ** $^{\circ}O_2$ **(Ψ αξις) ας πρεδιςτεδ ωιτη λοςαλ σινκ-σουρςε ρατιο (ΛΣΣΡ, Ξ αξις) μεασυρεδ ειτηερ υνδερ αμβιεντ** $^{\circ}O_2$ **λεελ (A) ορ ελεατεδ** $^{\circ}O_2$ **(B). Τηε τερμ** $A\mu\alpha\xi_{700}/A\mu\alpha\xi_{400}$ **ινδιςατες τηε ρατιο οφ οβσερατιονς ον πλαντς γροων ατ 700 ς. 400 μμολ μολ**$^{-1}$**. Φορ γενοτψπες ρεφερ το Ταβλε 1. Τηε 95% ςονφιδενςε ιντεραλ ις προιδεδ φορ τηε ςορρελατιονς ανδ ΣΕΜ ερρορ βαρς αρε προιδεδ φορ εαςη γενοτψπε. Εξπ. 1, πηψτοτρον.**

Exp. 2: LSSR predicts e-CO_2 response also when measured at ambient CO_2 level

In Exp. 2 we tested 17 highly diverse rice genotypes (including the five used by Fabre et al. 2020). A significant negative correlation was obtained between CO_2 response and LSSR in Exp. 2, both for $A_{\max}$ and grain yield, and both for LSSR measured under ambient and elevated CO_2 levels (Fig. 2). However, as in Exp. 1 the correlation was much stronger when LSSR was measured under elevated than under ambient CO_2 levels. Across the 17 genotypes, the LSSR measured at ambient CO_2 level predicted 35% of variation of the $A_{\max}$ response to elevated CO_2(40% for grain yield response). By contrast, the LSSR measured at elevated CO_2 predicted 67% of the $A_{\max}$ response (56% for grain yield response).

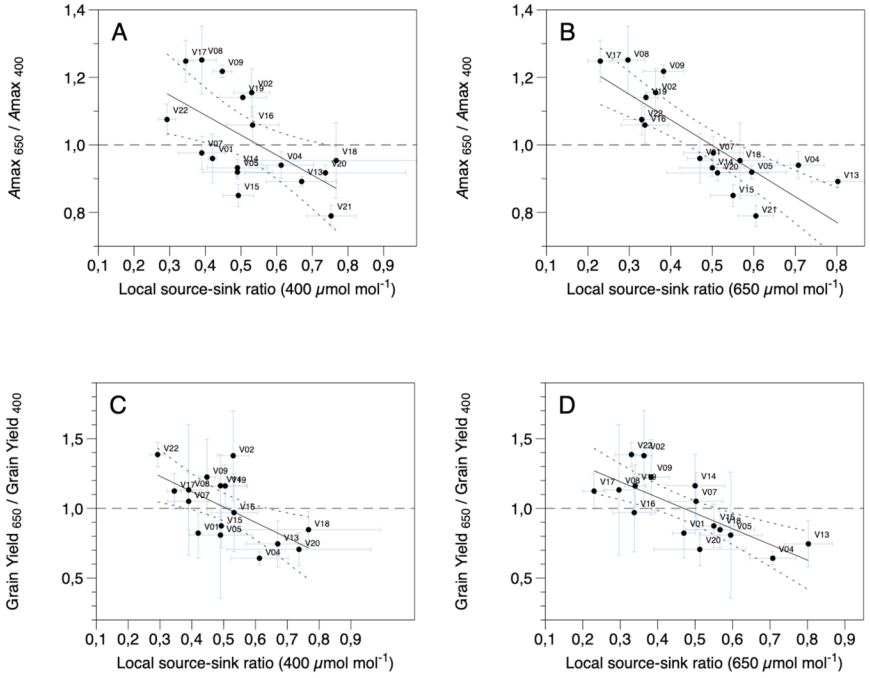

Fig. 2. Genotypic response of flag leaf $A_{\max}$ **(A, B) and plant grain yield (C,D) to elevated**

CO_2 (Y axis) as predicted with local sink-source ratio (LSSR, X axis) measured either under ambient CO_2 level (Fig. A, C) or elevated CO_2(B, D). For genotypes refer to Table 1. The 95% confidence interval is provided for the correlations and SEM error bars are provided for each genotype. Exp. 2, greenhouse.

Various source and sink related traits participate in the response to elevated CO_2

Observed trait means and analysis of variance (ANOVA) are presented in Table S2 (supplemental materials). Figure 3 presents correlation heatmaps for the observed traits under ambient (A) and elevated (B) CO_2 levels, whereby the CO_2 effect onA_{max} and grain yield (trait variation) was included in both matrices. The A_{max} and grain yield variation between the two environments were positively correlated (P<0.01) with each other, and both were negatively correlated with LSSR as also shown in Fig. 2. They were similarly correlated with two other calculated, potential, proxy traits for source-sink ratio: the LSSR(sink) that uses the product of panicle spikelet number and the genotypic filled-grain weight (instead of just the spikelet number) as an estimate of the sink; and [LSSR(sink) * SPAD] which factors the area leaf chlorophyll content into the equation to strengthen the source term (Table S1). In fact, A_{max} and the electron transport rate ETR were positively correlated with SPAD (P<0.01) under ambient but not under elevated CO_2 levels (Fig. 3). The ETR was negatively correlated with SLA (P<0.05) in both environments. Leaf sucrose concentration was weakly, positively correlated (P<0.05) with the tentative proxy traits LSSR, LSSR(sink) and LSSR(sink)*SPAD under elevated CO_2, but not ambient CO_2 level. The spikelet number per panicle was positively correlated with flag leaf ETR (P<0.05). The SPAD chlorophyll content was generally negatively correlated with SLA but positively with most of the other morphological traits such as leaf dimensions, panicle size traits and total shoot dry matter.

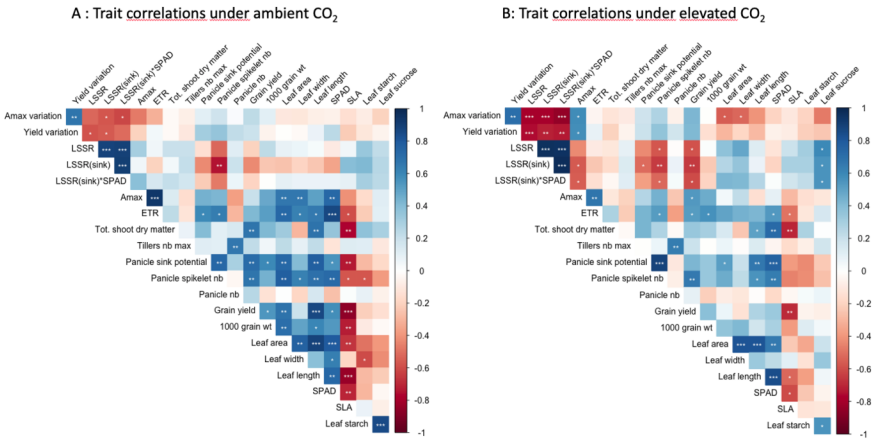

Fig. 3. Correlation heatmap for traits measured under ambient CO_2 (left) or elevated CO_2 level (right). The variables A_{max} variation and yield variation (ratios for elevated over ambient CO_2) are common to both heatmaps. Color codes express variation of R, with P<0.05 (*), P<0.01 (**) or P<0.001 (***). Exp. 2, greenhouse.

Principal component analysis (PCA, Fig. 4) opposed the tentative proxy traits LSSR, LSSR(sink) and LSSR(sink)*SPAD to the CO_2effect on A_{max} and grain yield variation in both CO_2 treatments, indicating negative correlation on both dimensions of the PCA.

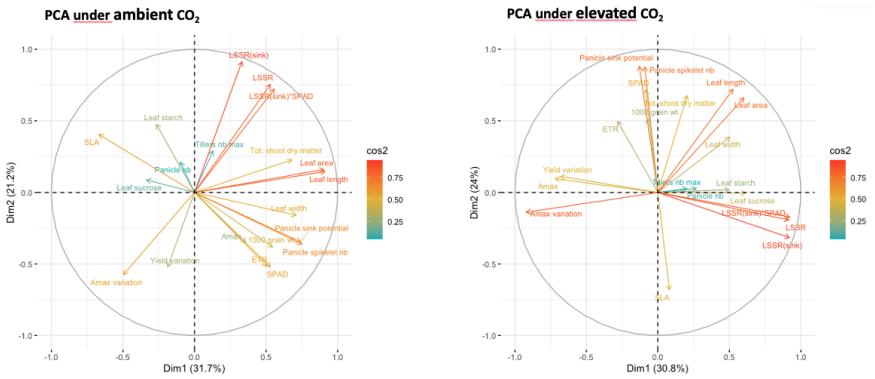

Fig. 4. Two-dimensional principal component analyses (PCA) for the same variables as in Fig. 3. Cos2 levels express the quality of the representation. Exp. 2, greenhouse.

Which tentative proxy traits did best predict A_{max} response to elevated CO_2?

The previously proposed proxy trait LSSR (Fabre et al., 2020), when measured under ambient CO_2 level, predicted 35% (R^2=0.35) of the genotypic variation of elevated-CO_2effects on A_{max} (Fig. 2A). When spikelet number, which is the sink term of LSSR, was replaced with [spikelet number * mean filled grain weight], resulting in the $LSSR_{sink}$term, the prediction increased to 45% (Fig. 5A). The prediction increased further to 50% when the source term flag leaf area was multiplied with SPAD chlorophyll content, resulting in the term $LSSR_{sink}$*SPAD (Fig. 5B).

Fig. 5. Prediction of genotypic response of flag leafA_{max} to elevated CO_2 (Y axis) using improved variants of the proxy trait LSSR measured under ambient CO_2 level. A: Proxy trait $LSSR_{sink}$(400); B: Proxy trait $LSSR_{sink}$*SPAD (400). Calculations of proxy traits are detailed in Table S1. The 95% confidence interval is provided for the correlations. Exp. 2, greenhouse.

Are the tentative proxy traits themselves affected by CO_2 level?

Linear correlations for the three tentative proxy traits measured under elevated vs. ambient CO_2 levels were similar among the traits (Fig. 6A). Overall across the 17 genotypes, the slope was near 1, indicating the absence of a generic effect. However, with R^2 values between 0.5 and 0.6, there was considerable scatter, and the SEM error bars indicated that for some genotypes, there was an effect of CO_2 level on the proxy trait value.

In fact, there generally was a clear negative trend (in some cases significant at $P<0.05$) in the relationship between the plasticity of the proxy traits (expressed as the difference between elevated and ambient CO_2 levels) vs. the *Amax* or grain yield ratio observed between the CO_2 levels (Fig. S1, supplemental materials). Consequently, those genotypes that had a reduced proxy trait value under e-CO_2 due to phenotypic plasticity showed a smaller *Amax* or yield gain under e-CO_2.

Correlations across genotypes of the other measured variables under elevated vs. ambient CO_2 levels are shown in Fig. S2 (supplemental materials).

Fig. 6. Linear correlations indicating the degree of conservation of three proxy traits between ambient and elevated CO_2 levels. A, LSSR; B, $LSSR_{sink}$; C, $LSSR_{sink}$*SPAD. The 95% confidence interval is provided for correlations and SEM error bars are provided for each genotype. Exp. 2, green house.

Discussion

The hypothesis was confirmed

The two experiments we reported leave no doubt that flag leaf$A_{\max}$ of rice under elevated [CO_2], under the irrigated experimental conditions, is partly controlled by genotypic source-sink relationships. This was initially reported by Fabre et al. (2020) for 5 genotypes and here in Exp.1 for 14 genotypes and in Exp.2 for 17 genotypes. A similar response to e-CO_2 of grain yield was reported by Fabre et al. (2020) and was also found here in Exp.2. The LSSR as a proxy trait for source-sink ratio is thus indicative of genotypic variation of acclimation of photosynthesis under e-CO_2. This acclimation, where present, consists of a downregulation of the maximum leaf photosynthesis capacity level ($A_{\max}$), which affects grain yield (White *et al.* , 2016; Fabre *et al.* , 2020; Dingkuhn *et al.* , 2020; Gao *et al.* , 2021).

Importantly, the two constituent traits of the LSSR, flag leaf area and panicle spikelet number, had either no or only a weak correlation with the e-CO_2 response of $A_{\max}$ or grain yield (Fig. 3). Only the ratio of the two traits was predictive, indicating that the underlying mechanism was indeed related to sink-source relationships, and not to a single morphological trait that might be correlated with acclimation for different reasons. On this basis, we suggest it to be likely that the "true" sink-source ratio of the plant, which would take into account the sums of all its source and sink activities (as opposed to a single leaf's area and panicle's spikelet number) would be more predictive than LSSR. Thus, hypothetically, better-performing proxy traits for e-CO_2response should exist but may be more difficult to measure.

We gave a greater emphasis to flag leaf A max than to yield or biomass response because i) according to this study's hypothesis, photosynthesis is directly affected by e-CO_2 acclimation whereas biomass and grain production are indirectly affected; and ii) our two samples of genotypes represented genetic diversity for LSSR and included very low-yielding accessions. It can be expected that in tall-traditional cultivars which partition comparatively little photosynthate to grains, yield is only loosely determined by leaf photosynthetic rates. A subsequent, similar study should address a panel of high-yielding genetic materials.

Why were proxy traits for CO_2 response more predictive when measured at elevated [CO_2]?

For purposes of practical applications of LSSR in plant phenotyping and selection or breeding for rice CO_2 response, it is sobering that in both our experiments the LSSR measured under elevated [CO_2] was much more predictive than that measured under ambient [CO_2]. (In Exp.1, the latter was not predictive at all, Fig. 1A.) Given our finding that genotypic LSSR was highly constitutive between CO_2 levels, with a slope of 1 for the linear regression, we can exclude that this difference was caused by a common adaptive-plasticity response of the LSSR trait for the population as a whole. However, those genotypes that showed a reduction in LSSR (or values of alternative proxy traits discussed further down) under elevated [CO_2] tended to have greater gain in $A_{\max}$ and grain yield under elevated [CO_2]. Although this trend was mostly not significant statistically, it is clear that variable phenotypic plasticity among the genotypes was responsible for the greater predictability of e-CO_2 response with proxy traits measured under elevated [CO_2].

Scope for improvement of proxy traits to better predict CO_2 response

Specifically to improve the predictability of genotypic$A_{\max}$ gains under e-CO_2 we attempted to refine the indices used as proxy traits, particularly as measured under ambient CO_2 conditions. Among the individual traits measured in Exp.2, there were none stood out as candidates according to PCA (Fig. 4). However, physiological reasoning suggested that the source term of LSSR should be improved by including the areal leaf chlorophyll content (easily measured with SPAD, thereby factoring in implicitly leaf thickness), and the sink term with the mean filled grain weight (routinely measured by breeders). This increased the$A_{\max}$-ratio prediction from 35% to 50% of the observed variation (Fig. 5). This, however, remained significantly inferior to the predictability using proxy traits measured under elevated [CO_2], a condition unavailable to breeders.

Further improvement of the predictability of genotypic e-CO_2 response, particularly for grain yield or biomass, may require a more fundamental rethinking of the proxy concept, which does not necessarily have to be based on morphology. Leaf sucrose accumulation, commonly pronounced in the afternoon (Kölling *et al.* , 2015; Fabre *et al.* , 2019, 2020), has been described as indicating sink limitation (Lemoine *et al.* , 2013; White *et al.* , 2016; Burnett *et al.* , 2016; Sonnewald and Fernie, 2018) and causing feedback inhibition of photosynthesis (Huber and Huber, 1992; Moore *et al.* , 1999; Iglesias *et al.* , 2002; Paul and Pellny, 2003;

Fabre *et al.* , 2019) but it was of limited predictive value in our study. We did not measure here fluorescence-based, diagnostic variables of the photosynthetic system (except the electron transport rate ETR, Fig. 3) which might be incorporated in observable, predictive indices. The disadvantage of such transient variables is their sensitivity to rapid environmental fluctuations, as opposed to morphology. On the sink side, we know of no readily deployable measurements of actual physiological demand for assimilates, and breeders are probably more comfortable with morphological sink proxies. More research on the processes involved in CO_2 acclimation of photosynthesis may open other avenues.

Lastly, it should be noted that sink-source relations exist also during vegetative growth and affect pre-floral biomass accumulation under e-CO_2 conditions (Dingkuhn et al., 2021). For example, genotypic tillering potential has been shown to contribute positively to crop e-CO_2 response in rice (Ziska et al., 2013; Kadam et al., 2019). Genotypic branching capacity in soybean has a similar effect (Kumagai et al., 2015). The search for predictive proxy traits with regards to vegetative biomass production is largely virgin territory.

A necessary step towards future application of proxy traits: Field validation

The present study was conducted in controlled environments. As its objective was to identify easily measurable proxy traits for genotypic response to e-CO_2 to be used for phenotyping a large number of genotypes in the context of crop improvement, a field validation will be necessary to validate their predictive potential when measured both in current and elevated-CO_2 environments. Ideally, this should be done in an existing FACE experimental setup, using a population that represents both genetic/phenotypic diversity and a large number of high-yielding materials. Hasegawa (2013) demonstrated in a FACE trial in Japan that diverse levels of CO_2acclimation occur among modern, high-yielding cultivars.

For future applications in crop breeding, direct selection for the proxy traits is possible if measurement costs and complexity are limited. It is also conceivable that once suitable proxy traits are found and field validated, they can be applied to larger genetic panels for association studies to identify molecular markers for them. Such markers, if performing well, might be more readily adopted by breeders than physiological measurements.

References

Burnett AC, Rogers A, Rees M, Osborne CP . 2016. Carbon source-sink limitations differ between two species with contrasting growth strategies: Source-sink limitations vary with growth strategy. Plant, Cell & Environment **39** , 2460–2472.

Cai C, Li G, Di L, *et al.* 2020. The acclimation of leaf photosynthesis of wheat and rice to seasonal temperature changes in T-FACE environments. Global Change Biology **26** , 539–556.

Dingkuhn M, Luquet D, Fabre D, Muller B, Yin X, Paul MJ . 2020. The case for improving crop carbon sink strength or plasticity for a CO2-rich future. Current Opinion in Plant Biology **56** , 259–272.

Fabre D, Adriani DE, Dingkuhn M, Ishimaru T, Punzalan B, Lafarge T, Clément-Vidal A, Luquet D . 2016. The qTSN4 Effect on Flag Leaf Size, Photosynthesis and Panicle Size, Benefits to Plant Grain Production in Rice, Depending on Light Availability. Frontiers in Plant Science**7** .

Fabre D, Dingkuhn M . 2022. Why is rice Amax (at saturating CO2) more heritable than Asat (at ambient CO2)? A commentary on Acevedo-Siaca et al. (2021). Plant Breeding **141** , 542–545.

Fabre D, Dingkuhn M, Yin X, Clément-Vidal A, Roques S, Soutiras A, Luquet D . 2020. Genotypic variation in source and sink traits affects the response of photosynthesis and growth to elevated atmospheric CO2. Plant, Cell & Environment **43** , 579–593.

Fabre D, Yin X, Dingkuhn M, Clement-Vidal A, Roques S, Rouan L, Soutiras A, Luquet D . 2019. Is triose phosphate utilization involved in the feedback inhibition of photosynthesis in rice under conditions of sink limitation? Journal of Experimental Botany **70** , 5773–5785.

Gao B, Hu S, Jing L, Niu X, Wang Y, Zhu J, Wang Y, Yang L . 2021. Alterations in Source-Sink Relations Affect Rice Yield Response to Elevated CO2: A Free-Air CO2 Enrichment Study. Frontiers in Plant Science **12** .

Hasegawa T, Sakai H, Tokida T, *et al.* 2013. Rice cultivar responses to elevated CO2 at two free-air CO2 enrichment (FACE) sites in Japan. Functional Plant Biology **40** , 148.

Hasegawa T, Sakai H, Tokida T, Usui Y, Yoshimoto M, Fukuoka M, Nakamura H, Shimono H, Okada M . 2016. Rice Free-Air Carbon Dioxide Enrichment Studies to Improve Assessment of Climate Change Effects on Rice Agriculture. Advances in Agricultural Systems Modeling. Improving Modeling Tools to Assess Climate Change Effects on Crop Response. Madison, WI: American Society of Agronomy, Crop Science Society of America, and Soil Science Society of America, Inc., 45–68.

Huber SC, Huber JL . 1992. Role of Sucrose-Phosphate Synthase in Sucrose Metabolism in Leaves. Plant Physiology **99** , 1275–1278.

Iglesias DJ, Lliso I, Tadeo FR, Talon M . 2002. Regulation of photosynthesis through source: sink imbalance in citrus is mediated by carbohydrate content in leaves. Physiologia Plantarum **116** , 563–572.

Impa SM, Raju B, Hein NT, Sandhu J, Prasad PVV, Walia H, Jagadish SVK . 2021. High night temperature effects on wheat and rice: Current status and way forward. Plant, Cell & Environment **44** , 2049–2065.

Jagadish SVK, Bahuguna RN, Djanaguiraman M, Gamuyao R, Prasad PVV, Craufurd PQ . 2016. Implications of High Temperature and Elevated CO2 on Flowering Time in Plants. Frontiers in Plant Science **7** .

Jagadish SVK, Murty MVR, Quick WP . 2015. Rice responses to rising temperatures – challenges, perspectives and future directions. Plant, Cell & Environment **38** , 1686–1698.

Kadam NN, Jagadish KSV, Struik PC, van der Linden GC, Yin X. 2019. Incorporating genome-wide association into eco-physiological simulation to identify markers for improving rice yields. *J. Exp. Bot.* 70, 2575-2586.

Kolling K, Thalmann M, Muller A, Jenny C, Zeeman SC . 2015. Carbon partitioning in Arabidopsis thaliana is a dynamic process controlled by the plants metabolic status and its circadian clock. Plant, Cell & Environment **38** , 1965–1979.

Kumagai E, Aoki N, Masuya Y, Shimono H. 2015. Phenotypic Plasticity Conditions the Response of Soybean Seed Yield to Elevated Atmospheric CO_2 Concentration. *Plant Physiol* . 169, 2021–2029.

Kumar U, Quick WP, Barrios M, Sta Cruz PC, Dingkuhn M . 2017. Atmospheric CO2 concentration effects on rice water use and biomass production. PLoS ONE **12** .

Lemoine R, Camera SL, Atanassova R, *et al.* 2013. Source-to-sink transport of sugar and regulation by environmental factors. Frontiers in Plant Science **4** , 272.

Liu S, Waqas MA, Wang S, Xiong X, Wan Y . 2017. Effects of increased levels of atmospheric CO2 and high temperatures on rice growth and quality. PLOS ONE **12** , e0187724.

Liu H, Yang L, Wang Y, Huang J, Zhu J, Yunxia W, Dong G, Liu G . 2008. Yield formation of CO2-enriched hybrid rice cultivar Shanyou 63 under fully open-air field conditions. Field Crops Research**108** , 93–100.

Lv C, Huang Y, Sun W, Yu L, Zhu J . 2020. Response of rice yield and yield components to elevated [CO2]: A synthesis of updated data from FACE experiments. European Journal of Agronomy **112** , 125961.

Mai W, Abliz B, Xue X . 2021. Increased Number of Spikelets per Panicle Is the Main Factor in Higher Yield of Transplanted vs. Direct-Seeded Rice. Agronomy **11** , 2479.

McClain AM, Cruz JA, Kramer DM, Sharkey TD . 2023. The time course of acclimation to the stress of triose phosphate use limitation. Plant, Cell & Environment **46** , 64–75.

Moore BD, Cheng S-H, Sims D, Seemann JR . 1999. The biochemical and molecular basis for photosynthetic acclimation to elevated atmospheric CO2. Plant, Cell & Environment **22** , 567–582.

Nakano H, Yoshinaga S, Takai T, *et al.* 2017. Quantitative trait loci for large sink capacity enhance rice grain yield under free-air CO2 enrichment conditions. Scientific Reports **7** , 1827.

Paul MJ, Pellny TK . 2003. Carbon metabolite feedback regulation of leaf photosynthesis and development. Journal of Experimental Botany**54** , 539–547.

Pomeranz Y, Meloan CE . 1994. Enzymatic Methods. In: Pomeranz Y,, In: Meloan CE, eds. Food Analysis: Theory and Practice. Boston, MA: Springer US, 506–531.

Rebolledo MC, Pena AL, Duitama J, Cruz DF, Dingkuhn M, Grenier C, Tohme J . 2016. Combining Image Analysis, Genome Wide Association Studies and Different Field Trials to Reveal Stable Genetic Regions Related to Panicle Architecture and the Number of Spikelets per Panicle in Rice. Frontiers in Plant Science **7** , 1384.

Rohde, M.M. Floods and droughts are intensifying globally. *Nat Water* **1** , 226–227 (2023). https://doi.org/10.1038/s44221-023-00047-y

Sadok W, Jagadish SVK . 2020. The Hidden Costs of Nighttime Warming on Yields. Trends in Plant Science **25** , 644–651.

Seneweera S, Makino A, Hirotsu N, Norton R, Suzuki Y . 2011. New insight into photosynthetic acclimation to elevated CO2: The role of leaf nitrogen and ribulose-1,5-bisphosphate carboxylase/oxygenase content in rice leaves. Environmental and Experimental Botany**71** , 128–136.

Sharkey TD . 2019. Is triose phosphate utilization important for understanding photosynthesis? Journal of Experimental Botany**70** , 5521–5525.

Sheehy JE, Dionora MJA, Mitchell PL . 2001. Spikelet numbers, sink size and potential yield in rice. Field Crops Research **71** , 77–85.

Sonnewald U, Fernie AR . 2018. Next-generation strategies for understanding and influencing source-sink relations in crop plants. Current opinion in plant biology **43** , 63–70.

Wang D, Rianti W, Galvez F, van der Putten PEL, Struik PC, Yin X . 2022. Estimating photosynthetic parameter values of rice, wheat, maize and sorghum to enable smart crop cultivation. Crop and Environment.

White AC, Rogers A, Rees M, Osborne CP . 2016. How can we make plants grow faster? A source–sink perspective on growth rate. Journal of Experimental Botany **67** , 31–45.

Xiong D, Yu T, Liu X, Li Y, Peng S, Huang J . 2015. Heterogeneity of photosynthesis within leaves is associated with alteration of leaf structural features and leaf N content per leaf area in rice. Functional Plant Biology **42** , 687–696.

Yin X, Busch FA, Struik PC, Sharkey TD . 2021. Evolution of a biochemical model of steady-state photosynthesis. Plant, Cell & Environment **44** , 2811–2837.

Ziska LH, Tomecek MB, Gealy DR. 2013. Assessment of cultivated and wild, weedy rice lines to concurrent changes in CO_2concentration and air temperature: determining traits for enhanced seed yield with increasing atmospheric CO_2. *Functional Plant Biology* **41** , 236-243.

Table S1. Measured and calculated variables

Variable name	Definition	Unit	Calculation
Amax	Flag leaf light & CO_2 saturated photosynthesis	µmol m^{-2} s^{-1}	n.a.
Amax variation	Rel. *Amax* (e-CO_2/ambient)	unitless	*Amax* (e-$CO_{2)}$ / *Amax* (ambien
Yield	Grain yield	g $plant^{-1}$	
Yield variation	Rel. yield (e-CO_2 / ambient)	unitless	Yield (e-$CO_{2)}$ / yield (ambient)
ETR	Electron transport rate	µmol mol^{-1} s^{-1}	ETR = φPSII × PAR × 0.84 ×
Leaf area	Flag leaf area	cm^2	Leaf area * Leaf width * 0.725
Leaf length	Flag leaf length	cm	n.a.
Leaf width	Flag leaf width	cm	n.a.
Leaf sucrose	Flag leaf [sucrose]	mg g^{-1}	n.a.
Leaf starch	Flag leaf [starch]	mg g^{-1}	n.a.
Panicle spikelet nb	Spikelets nb per panicle	unitless	n.a.
Panicle sink potential	Product of spikelet nb & filled grain weight	g	Panicle spikelet nb * 1000 grain
SLA	Specific leaf area	cm^2 g^{-1}	Flag leaf area / dry weight
SPAD	Flag leaf areal chlorophyll content	unitless	n.a.
1000 grain wt	Dry wt of 1000 filled grains	g	n.a.
Tiller nb max	Tiller nb/plant	unitless	n.a.
Tot. shoot dry matter	Aboveground dw at maturity	g $plant^{-1}$	n.a.
Proxy traits:			
LSSR	Local source-sink ratio	unitless	Flag leaf area / Panicle spikelet
$LSSR_{sink}$	LSSR based on sink potential	unitless	Flag leaf area / (Panicle spikele
$LSSR_{sink}$*SPAD		unitless	(Flag leaf area * SPAD) / (Pani

n.a., not applicable

Table S2. Means and ANOVA of observed variables by genotype and treatment. Exp. 2, greenhouse.

	Amax	ETR	LSSR	LSSR(sink)	LSSR(sink)*SPAD	Tot. shoot dry matter	Tillers nb max	Panicle sink potential	Panicle spikelet nb.	Panicle nb	1000 grain wt	Leaf area	SPAD	SLA	Leaf starch	Leaf sucrose
	µmol m^{-2} s^{-1}	µmol m^{-2} s^{-1}	number	number	number	g	number	number	number	number	g	cm^2	number	cm^2 g^{-1}	mg g^{-1} DM	mg g^{-1} DM
V01*Ambiant	21,3 abcde	147,1 abcdef	0,42 abcdefg	0,017 abcde	0,75 bcd	42,5 fghij	17,0 hijkl	3852,1 abcdefg	156,0 bcdefg	11,7 ef	24,5 abcd	65,6 bcdefgh	44,1 abcdef	287,4 bcdefghi	1,0 c	70,5 abcd
V01*High CO2	22,3 abcde	161,1 abc	0,47 abcdefg	0,019 abcde	0,85 bcd	52,9 efghij	18,5 ghijkl	4016,7 abcde	162,7 abcdefg	11,5 ef	25,0 abc	75,6 bcdef	44,9 abcdef	357,1 abc	1,3 c	69,7 abcd
V02*Ambiant	21,3 abcdef	131,2 abcdef	0,53 abcdefg	0,024 abcde	1,01 bcd	84,6 cdef	26,5 cdefghij	1946,7 efghi	88,2 efgh	19,5 bcdef	22,0 cdefghijkl	42,6 efghij	42,5 cdef	288,4 bcdefghi	11,7 abc	90,4 ab
V02*High CO2	24,6 abc	134,3 abcdef	0,36 abcdefg	0,016 abcde	0,72 bcd	92,3 bcde	31,7 bcdefg	2426,5 defghi	110,0 defgh	25,8 ab	22,2 cdefghijk	39,0 fghij	44,4 abcdef	274,2 cdefghi	11,0 abc	80,7 abcd
V04*Ambiant	20,0 abcdef	99,1 cdefgh	0,61 abcdefg	0,027 abcde	1,03 bcd	59,3 efghij	19,3 ghijkl	909,3 l	40,3 h	12,5 ef	22,1 cdefghijkl	24,0 ij	37,7 f	331,0 abcdefgh	12,4 abc	92,1 a
V04*High CO2	18,8 abcdef	97,7 cdefgh	0,71 abcdefg	0,031 abcde	1,25 bcd	67,0 defghi	20,5 fghijkl	1259,5 l	55,8 gh	12,8 ef	23,1 bcdefgh	38,0 fghij	40,2 cdef	313,8 abcdefgh	19,9 a	88,1 abc
V05*Ambiant	18,3 bcdef	88,1 efgh	0,49 abcdefg	0,027 abcde	1,07 bcd	42,8 fghij	39,0 abc	1295,4 l	70,3 fgh	16,8 bcdef	18,8 lm	33,5 ghij	39,5 def	391,3 a	9,6 abc	79,6 abcd
V05*High CO2	16,8 def	83,5 fgh	0,60 abcdefg	0,032 abcde	1,33 bcd	46,3 efghij	45,8 a	1459,6 ghi	79,3 fgh	23,3 abcd	18,1 m	45,0 defghij	41,7 cdef	351,8 abcd	5,6 bc	72,5 abcd
V07*Ambiant	18,9 abcdef	97,3 cdefgh	0,50 abcdefg	0,025 abcde	0,98 bcd	44,5 efghij	26,0 defghijk	2234,7 defghi	111,0 defgh	23,3 abcd	19,4 klm	50,1 cdefghij	40,2 cdef	332,7 abcdefg	1,5 c	60,8 abcd
V07*High CO2	18,5 bcdef	90,8 defgh	0,39 abcdefg	0,019 abcde	0,84 bcd	59,3 efghij	30,8 bcdefg	3266,5 bcdefghi	162,3 abcdefg	30,3 a	20,9 efghijklm	63,2 bcdefghi	43,6 bcdef	304,4 abcdefghi	3,3 c	61,3 abcd
V08*Ambiant	16,3 ef	61,1 h	0,39 abcdefg	0,020 abcde	0,78 bcd	28,0 hij	13,5 kl	1413,3 hi	73,3 fgh	10,7 ef	19,0 klm	27,5 hij	38,4 ef	364,5 ab	1,6 c	57,3 cd
V08*High CO2	20,4 abcdef	66,6 gh	0,30 abcdefg	0,015 abcde	0,63 bcd	34,9 ghij	14,5 jkl	1501,2 fghi	74,0 fgh	10,5 ef	19,6 ijklm	23,0 j	41,2 cdef	348,3 abcde	2,1 c	52,4 d
V09*Ambiant	19,9 abcdef	123,5 abcdefgh	0,45 abcdefg	0,020 abcde	0,90 bcd	48,9 efghij	19,3 ghijkl	2719,6 cdefghi	120,3 cdefgh	15,0 cdef	23,5 abcdefgh	53,4 cdefghij	45,0 abcdef	273,7 cdefghi	1,7 c	73,0 abcd
V09*High CO2	24,2 abcd	142,4 abcdef	0,38 abcdefg	0,017 abcde	0,73 bcd	50,8 efghij	22,8 efghijkl	3234,1 bcdefghi	143,0 bcdefgh	16,5 bcdef	21,4 defghijklm	55,3 bcdefghi	43,3 bcdef	260,0 efghi	1,8 c	69,3 abcd
V13*Ambiant	26,3 a	167,6 ab	0,67 abcdefg	0,029 abcde	1,33 bcd	19,6 ij	28,8 bcdefghi	2832,2 cdefghi	121,3 cdefgh	12,3 ef	22,9 bcdefghi	77,3 bcdef	46,7 abcde	339,4 abcdef	1,1 c	65,5 abcd
V13*High CO2	23,5 abcde	141,3 abcdef	0,80 abcdefg	0,034 abcde	1,54 bcd	25,8 hij	34,0 abcde	2797,2 cdefghi	119,8 cdefgh	16,3 bcdef	23,8 abcdefg	95,2 b	44,8 abcdef	293,8 bcdefghi	2,9 c	79,1 abcd
V14*Ambiant	19,9 abcdef	123,5 abcdefgh	0,49 abcdefg	0,022 abcde	0,96 bcd	53,6 efghij	32,8 bcdef	2800,2 cdefghi	126,0 cdefgh	20,5 abcde	22,0 cdefghijkl	57,0 bcdefghij	44,2 abcdef	300,8 bcdefghi	3,5 c	73,2 abcd
V14*High CO2	18,6 bcdef	101,3 cdefgh	0,50 abcdefg	0,022 abcde	0,99 bcd	56,6 efghij	40,3 ab	3172,5 bcdefghi	142,8 bcdefgh	20,5 abcde	22,5 cdefghij	68,6 bcdefg	44,2 abcdef	280,4 bcdefghi	5,9 bc	83,7 abcd
V15*Ambiant	21,9 abcde	165,8 ab	0,49 abcdefg	0,024 abcde	1,15 bcd	118,1 abc	13,5 kl	2467,8 defghi	121,0 cdefgh	12,0 ef	20,4 hijklm	58,5 bcdefghij	48,2 abc	246,5 ghi	5,8 bc	83,1 abcd
V15*High CO2	20,3 abcdef	159,2 abc	0,55 abcdefg	0,027 abcde	1,27 bcd	112,1 abcd	13,3 l	2697,2 cdefghi	132,3 cdefgh	12,8 ef	20,4 hijklm	71,8 bcdefg	47,3 abcd	250,6 fghi	10,3 abc	79,4 abcd
V16*Ambiant	22,6 abcde	157,1 abc	0,53 abcdefg	0,020 abcde	0,95 bcd	121,7 abc	32,0 bcdef	4625,9 abcd	175,8 abcdef	15,3 cdef	26,5 a	89,8 bc	47,1 abcd	215,7 i	2,9 c	61,4 abcd
V16*High CO2	23,9 abcde	166,6 ab	0,34 abcdefg	0,013 abcde	0,60 bcd	118,1 abc	33,8 abcde	4546,9 abcd	172,8 abcdef	14,8 def	26,2 ab	58,2 bcdefghi	46,4 abcde	221,0 i	6,4 bc	59,2 bcd
V17*Ambiant	19,3 abcdef	119,0 abcdefgh	0,35 abcdefg	0,015 abcde	0,68 bcd	67,1 defghi	37,5 abcd	4225,1 abcde	189,3 abcde	19,0 bcdef	22,1 cdefghijk	64,4 bcdefgh	44,0 bcdef	279,9 bcdefghi	3,9 c	69,4 abcd
V17*High CO2	24,0 abcd	139,5 abcdef	0,23 abcdefg	0,010 abcde	0,47 bcd	69,6 defgh	41,0 ab	4967,4 abc	222,5 abc	17,5 bcdef	22,5 cdefghij	50,0 cdefghij	44,6 abcdef	242,2 hi	4,6 c	74,2 abcd
V18*Ambiant	22,3 abcde	153,2 abcd	0,76 abcdefg	0,034 abcde	1,44 bcd	64,3 defghi	20,0 fghijkl	2021,5 efghi	89,3 efgh	15,5 bcdef	22,8 cdefghi	61,9 bcdefghij	42,3 cdef	259,7 efghi	3,5 c	86,3 abc
V18*High CO2	21,2 abcdef	148,5 abcde	0,57 abcdefg	0,025 abcde	1,08 bcd	80,9 cdefg	26,0 defghijk	2081,9 efghi	92,0 efgh	16,0 bcdef	22,5 cdefghij	50,5 cdefghij	43,2 bcdef	262,5 defghi	5,5 bc	79,3 abcd
V19*Ambiant	21,2 abcdef	125,6 abcdefg	0,50 abcdefg	0,021 abcde	1,00 bcd	90,1 bcdef	19,0 ghijkl	2975,0 cdefghi	123,3 cdefgh	12,8 ef	24,1 abcdef	60,2 bcdefghij	47,8 abcd	264,8 defghi	9,3 abc	80,9 abcd
V19*High CO2	24,1 abcd	140,5 abcdef	0,34 abcdefg	0,014 abcde	0,67 bcd	122,0 abc	20,5 fghijkl	4906,1 abc	203,3 abcd	13,8 def	24,2 abcde	65,3 bcdefgh	47,4 abcd	256,4 fghi	8,0 abc	66,2 abcd
V20*Ambiant	18,8 abcdef	133,7 abcdefgh	0,74 abcdefg	0,034 abcde	1,78 bcd	144,8 a	22,3 efghijkl	3135,6 bcdefghi	143,7 bcdefgh	10,0 ef	22,2 cdefghijk	83,1 bcd	52,7 a	245,2 ghi	1,0 c	72,4 abcd
V20*High CO2	17,3 cdef	128,0 abcdefg	0,51 abcdefg	0,024 abcde	1,22 bcd	147,9 a	28,5 bcdefghi	3797,6 abcdefgh	174,0 abcdef	13,5 def	21,6 defghijkl	80,2 bcde	51,2 ab	245,5 ghi	2,2 c	73,0 abcd
V21*Ambiant	18,4 bcdef	103,9 bcdefgh	0,75 abcdefg	0,034 abcde	1,39 bcd	150,0 a	27,5 cdefghi	5435,6 ab	247,8 ab	15,3 cdef	21,9 defghijkl	182,8 a	41,1 cdef	277,2 bcdefghi	5,5 bc	56,4 cd
V21*High CO2	14,6 f	90,3 defgh	0,60 abcdefg	0,028 abcde	1,18 bcd	134,5 ab	29,5 bcdefgh	5830,3 a	265,8 a	25,3 abc	NA	160,4 a	42,7 bcdef	268,2 cdefghi	17,4 ab	79,2 abcd
V22*Ambiant	23,3 abcde	172,9 a	0,29 abcdefg	0,014 abcde	0,66 bcd	15,6 j	14,8 jkl	3928,3 abcde	190,5 abcde	9,7 f	20,7 fghijklm	54,1 cdefghij	47,6 abcd	311,8 abcdefgh	2,1 c	74,6 abcd
V22*High CO2	25,0 ab	160,6 abc	0,33 abcdefg	0,016 abcde	0,72 bcd	15,3 j	16,8 ijkl	3883,6 abcdef	188,3 abcde	9,5 f	20,5 ghijklm	61,8 bcdefghij	44,4 abcdef	322,8 abcdefgh	2,2 c	72,8 abcd
variety	**<0,0001**	**<0,0001**	**<0,0001**	**<0,0001**	**<0,0001**	**<0,0001**	**<0,0001**	**<0,0001**	**<0,0001**	**<0,0001**	**<0,0001**	**<0,0001**	**<0,0001**	**<0,0001**	**<0,0001**	**<0,0001**
CO2 treatment	0,6	0,8	**0,0**	**0,0**	0,1	0,1	**<0,0001**	**0,0**	**0,0**	**0,0**	0,7	0,7	0,5	0,1	**0,0**	0,9
variety*CO2 treatment	**0,0**	0,8	0,3	0,3	0,4	0,8	0,9	0,9	0,9	0,1	0,5	**0,0**	0,8	0,2	0,3	0,4

Fig. S1. Correlations between A_{max} ratio (A, C, E) or grain yield ratio (B, D, F) for elevated vs. ambient CO_2, and the proxy trait difference between both CO_2 levels. Exp. 2, greenhouse.

Fig. S2. Correlations of observed traits between ambient CO_2 (X-axis) and elevated CO_2 (Y-axis) levels. Exp. 2, greenhouse.